ChemComm

Accepted Manuscript

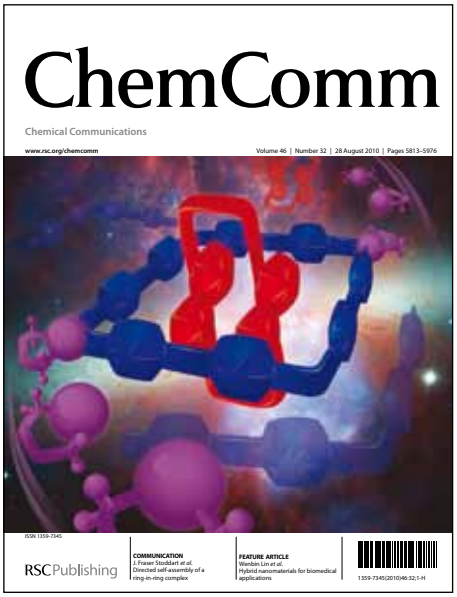

This is an *Accepted Manuscript*, which has been through the RSC Publishing peer review process and has been accepted for publication.

Accepted Manuscripts are published online shortly after acceptance, which is prior to technical editing, formatting and proof reading. This free service from RSC Publishing allows authors to make their results available to the community, in citable form, before publication of the edited article. This *Accepted Manuscript* will be replaced by the edited and formatted *Advance Article* as soon as this is available.

To cite this manuscript please use its permanent Digital Object Identifier (DOI®), which is identical for all formats of publication.

More information about *Accepted Manuscripts* can be found in the **Information for Authors**.

Please note that technical editing may introduce minor changes to the text and/or graphics contained in the manuscript submitted by the author(s) which may alter content, and that the standard **Terms & Conditions** and the **ethical guidelines** that apply to the journal are still applicable. In no event shall the RSC be held responsible for any errors or omissions in these *Accepted Manuscript* manuscripts or any consequences arising from the use of any information contained in them.

ChemComm

RSCPublishing

COMMUNICATION

Discrimination of lymph node metastases using desorption electrospray ionisation-mass spectrometry imaging

Cite this: DOI: 10.1039/xoxxoooooox

Abbassi-Ghadi N[1*] and Veselkov K[1*], Kumar S[1], Huang J[1], Jones E[1], Strittmatter N[1], Kudo H[2], Goldin R[2], Takáts Z[1†] and Hanna GB[1†]

Received ooth xx 20xx,
Accepted ooth xx 20x

DOI: 10.1039/xoxxoooooox

www.rsc.org/

Desorption electrospray ionisation mass spectrometry imaging (DESI-MSI) has been used for the identification of cancer within lymph nodes with accurate spatial distribution in comparison to gold standard matched immuno-histopathological images. The metabolic profile of the cancerous lymph nodes was similar to that of the primary tumour site.

Cancer has the ability to spread to its surrounding lymph nodes (LNs). Surgical removal remains the mainstay of treatment for the majority of cancers. Intra-operative identification of cancer, within LNs, otherwise known as lymph node metastases (LNM), can guide a surgeon on the appropriate amount of tissue to remove in order to give the patient the best chance of cure. The sentinel lymph node (SLN) is of primary importance as it is the gatekeeper to the rest of the regional LNs and is usually the first to harbour metastases. If metastases are found in the SLN the rest of the regional LNs are surgically removed due to a higher chance of them also being affected. Histopathological methods, including frozen section or touch imprint cytology are conventionally employed to fulfil the requirement for intra-operative LNM identification. The techniques rely on subjective assessment of cellular structure by a histopathologist and is prone to human error with consequent inter- and intra-observer variability.[1] Other methods such as serial step sectioning with immuno-histochemistry of paraffin embedded tissue has been shown to improve sensitivity for metastases in histopathological analysis, however its lengthier processing times make it unsuitable for intra-operative use.

Several novel non-histopathological techniques have been used to assess LN status intra-operatively. The use of one-step nucleic acid amplification (OSNA) assay,[2] real-time quantitative reverse-transcription polymerase chain reaction,[3] photo-acoustic tomographic imaging,[4] hand held positron emission tomography probe[5] and Raman spectroscopy[6] have been reported in the literature. The only method deemed suitable for clinical application is the OSNA assay, which relies on the molecular identification of cytokeratin-19 (CK19) mRNA. However, when processing a whole LN using the OSNA assay, several important diagnostic features including size, location and pattern of LNM and extra-capsular extension cannot be assessed.

Novel methods of tissue type identification, based on the chemical organisation of thin tissue slices, using mass spectrometry imaging (MSI) techniques have gained increasing interest.[7] The use of MALDI-MS for the identification of LNM, highlighted by areas varying protein intensities, has been shown in previous studies of patients with melanoma, and breast cancer.[8,9] Trace elements, detected by LA-ICPMS, have also been used to differentiate areas of metastases within LNs.[10] DESI-MS relies on similar principles of molecular differentiation, primarily detecting varying lipid intensities within the 600-900 *m/z* range. Specific areas of varying histology, including tumour versus normal surrounding tissue, have been demonstrated with false colour images in this context.[11,12] In comparison to other MSI techniques, DESI offers greater advantages with respect to clinical applications as it can be performed under ambient conditions with minimal sample preparation,[13,14] making it suitable for direct tissue analysis.

In this study, we report the first use of DESI-MSI for LNM identification. We also demonstrate similarities in the metabolic profile of the primary tumour to that of its LNM and illustrate how we can apply the molecular ion spectral pattern (MISP) of the primary tumor to objectively identify metastases within a LN of interest.

A total of 11 fresh tissue samples were retrieved from a human cancerous stomach specimen, after ethical approval from an institutional review board and informed written consent obtained by a licensed clinician. Eight of these tissue samples were LNs, with two containing macro-metastases, one containing micro-metastases and the other five being normal. The other 3 tissue samples were retrieved form the primary tumour site within the stomach. All the samples were stored at -80°C prior to cryo-sectioning at 15µm thickness and thaw mounted onto glass slides for DESI-MSI acquisition. DESI-MS analysis was performed using an Exactive fourier transform mass spectrometer (Thermo Fisher Scientific Inc., Bremen, Germany) controlled by XCalibur 2.1 software and operated in negative ion mode. The mass spectrometer was coupled

[a] *Department of Surgery and Cancer, Imperial College London, 10th Floor QEQM Wing, St Mary's Hospital, London, UK, W2 1NY*
[b] *Centre for Pathology, Imperial College London, 4th Floor Clarence Wing, St Mary's Hospital, London, UK, W2 1NY*
**Primary authors contributed equally to the work*
† Joint Corresponding authors contributed equally to the work
†Electronic Supplementary Information (ESI) available. See DOI: 10.1039/c000000x/

to a home-built DESI ion source, similar to a commercial source from Prosolia Inc. (Indianapolis, IN, USA) and set at a spatial resolution of 75µm. The MS instrument parameters and the geometric/solvent parameters of the DESI ion source are provided in the supplementary information (S1, ESI†).

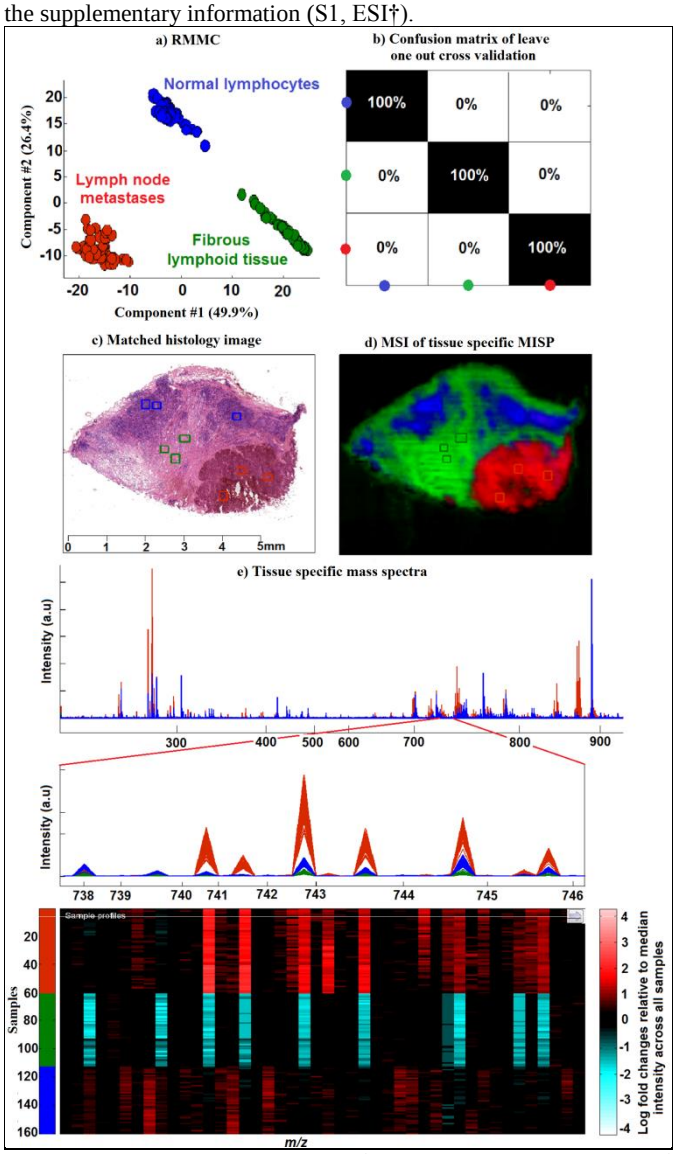

Figure 1: DESI-MSI data interrogation for a lymph node with evidence of macro-metastases

The same samples of LNs used for DESI-MSI were subsequently stained with haematoxylin & eosin and also immuno-stained with the anti-cytokeratin AE1:AE3 (Dako Ltd, Cambridgeshire, UK) to demonstrate areas of LNM with a red/brown stain. A histopathologist, specialising in stomach cancer assessment, blinded to the results of the DESI-MSI, examined the LNs for the presence of macro-metastases (>2mm) and micro-metastases (0.2mm-<2mm), using images obtained on a high resolution digital slide scanner (NanoZoomer2.0-HT, Hamamatsu City, Japan).

The MSI data was initially subjected to pre-processing which included peak detection, filtering of solvent/noise related peaks and variance stabilizing normalization with an in house bio-informatics platform (S2, ESI†).[15] Following the data pre-processing, the coordinates of DESI-MSI and its matched histology image were aligned by means of affine transformation, by maximizing the matching of tissue-related pixels between optical and MSI images. After image co-registration, regions of specific tissue types identified on the histology and the corresponding DESI-MSI were co-selected. The selected spectral profiles were subjected to supervised multivariate statistical analysis using recursive maximum margin criterion (RMMC) in order to extract tissue specific molecular ion spectral patterns (MISPs) for automated classification of all other tissue slide pixels.

DESI-MSI data interrogation, using our analytical framework, for a LN with evidence of macro-metastases is demonstrated in Fig. 1. Tissue specific mass spectra of normal lymphocytes (blue), fibrous lymphoid tissue (green) and LNM (red) were extracted from the co-registered histology and total ion MS images. The RMMC discriminant analysis shows a difference in the three tissue types using a weighted sum of molecular ion peak intensities, otherwise referred to as the MISP in this article (Fig. 1a). A region out cross validation confusion matrix (Fig. 1b) demonstrates 100% sensitivity and specificity for identifying the three different tissue types based on this association. A reconstructed MSI image (Fig. 1d) characterised by the MISPs of these tissue specific areas, demonstrates a similar spatial distribution to the matched immuno-histochemical image (Fig. 1c). Correct classifications of tissue types were also determined in a normal lymph node (S3, ESI†) and a lymph node containing micro-metastases (S4, ESI†).

We then compared the tissue specific mass spectra of the primary tumor, LN metastases, normal lymphocytes and fibrous lymphoid tissue of our full sample set using principal component analysis (PCA, see Fig. 2a). Three replicates of tissue specific mass spectra were determined for each sample by averaging out a hundred randomly selected spectra from the corresponding classified tissue object pixels. The tissue spectra were then subjected to the median fold change normalization, followed by log-based variance stabilizing transformation. The model was validated using 5 by 20 bi-cross-validation model which indicated that the three principal components were sufficient to explain overall similarities and differences between mass spectra of different tissue types (S5, ESI†). The PCA shows that the primary tumor is clustered closely to that of LNM, with separation from other normal lymph node tissue types. This is confirmed by Ward's hierarchical clustering analysis, which groups tumor-related profiles close together (Fig. 2b).

The distribution pattern and relative abundance of glycero-phospholipids in the 600-900 *m/z* range are the main discriminating features of the tissue specific mass spectra (S6, ESI†). Box plots in Fig. 2 demonstrate the relative abundance of a few selected species of glycero-phospholipids in primary tumour, LNM, fibrous lymphoid tissue and normal lymphocytes. Direct tissue DESI-MS/MS was performed using the ion trap of an Thermo LTQ XL mass spectrometer to correctly identify the selected glycero-phospholipids (S7a-d, ESI†). Empirical Bayes ANOVA (false discovery rate controlled at 5% level) showed that Phosphatidylethanolamine (PE) 18:2/18:0; and Phosphatidylinositol (PI) 18:2/18:0 are significantly higher, and Phosphatidylserine (PS) 20:4/18:0; and Phosphatidylinositol (PI) 18:0/20:4 are significantly lower in primary tumor tissue and LNM in comparison to normal lymph node tissue in this patient. These findings may be due to the inherent cellular differences in the specified tissue types and in part due to disruption of normal lipid synthesis in the cancer disease state, promoted by the de novo lipogenesis and disordered fatty acid synthase enzyme mechanism.[16] This is the first report of lipidomic comparison of primary tumour and its associated LNM, reinforcing the use of DESI-MSI as an important discovery tool for the investigation of glycerol-phospholipids in cancer.

In order to validate the metabolic similarities between the LNM and primary tumour we aimed to use the MISP from the primary tumor site to objectively identify metastases within a LN of interest. The average tumor specific MISP was found as a weighted sum of molecular ion intensities that discriminate primary tumour relative to normal LN tissues. Subsequently, these patterns were used to derive a normalized continuous score for every pixel in the LN of interest. The LN of interest was not used in the training set/model building process. The scores were visualized in a color coded manner with the colour intensity proportional to a score of a given pixel. Metastases are represented by a higher score relative to other normal LN tissue types (see Fig. 3).

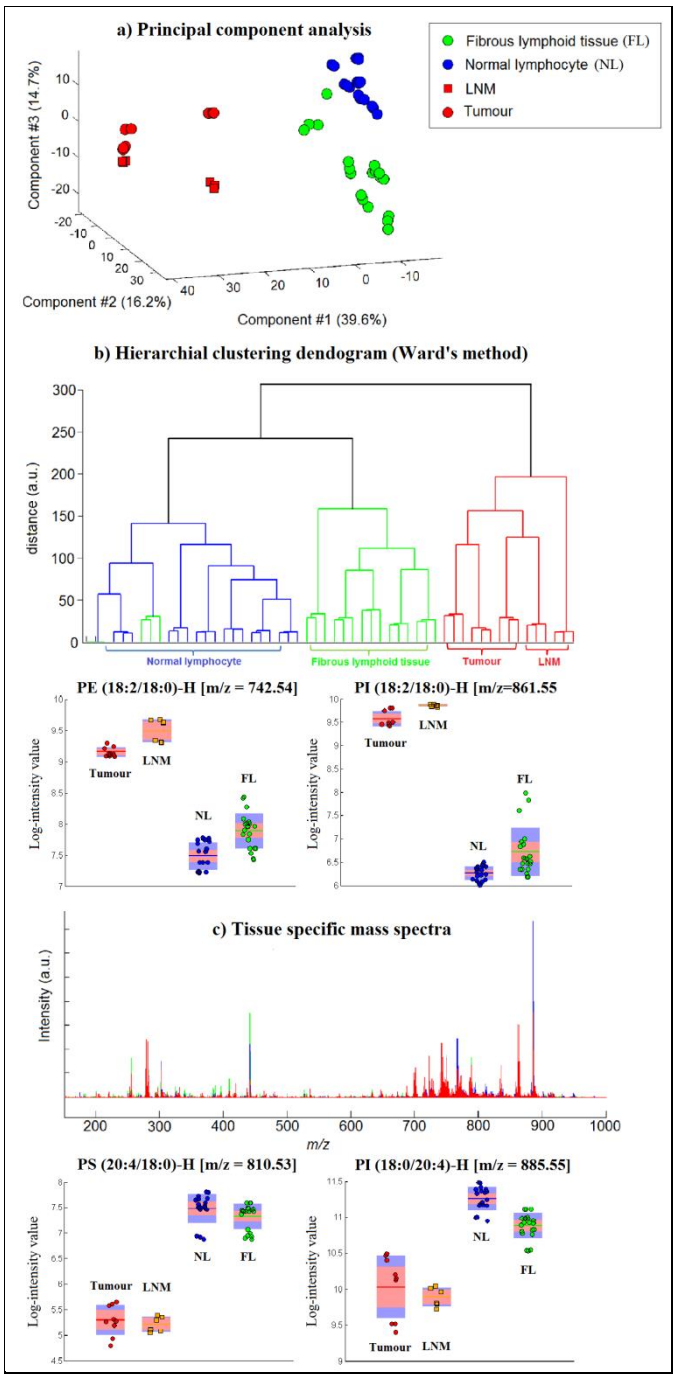

Figure 2: Comparative analysis of the MS profiles of primary tumor, lymph node metastases and normal lymph node tissues.

The objective identification of LNM based on the metabolic profile of the primary tumour has potential importance for clinical applications. For instance, a molecular profile of the primary tumour could be obtained pre-operatively through tissue biopsy or from a large pre-determined database of that particular tumor type, and used to find metastases in LNs at the time of the operation. This method would objectify the process of LNM identification and would mean that a histopathologist would not be required, thereby enhancing the intra-operative decision making capability of the surgeon. The SLN can be sampled at the start of an operation and processed by a technician as the surgeon continues to operate. Data acquisition would take approximately 10-20 minutes once the system is fully optimised and the lateral resolution reduced to 200µm, which is the lower limit of detection for micro-metastases. This is a realistic time frame for cancer operations, many of which take several hours. Once the surgeon is informed about the results, he/she can make a decision regarding clearing the rest of the regional LNs.

Very similar lipidomic spectral features can be determined by technologies such as rapid evaporation ionisation mass spectrometry (REIMS),[17] for in-vivo tissue identification of different types of metastases. However, ex-vivo analysis with DESI-MSI may be more suitable for the identification of LNM, as mass spectra can be obtained from discrete areas at a microscopic rather than a macroscopic level with REIMS, which would improve the chances of accurately identifying micro-metastases. Furthermore, results can be corroborated by histopathological assessment post-operatively, as the tissue sections remain structurally unaltered by DESI-MSI.

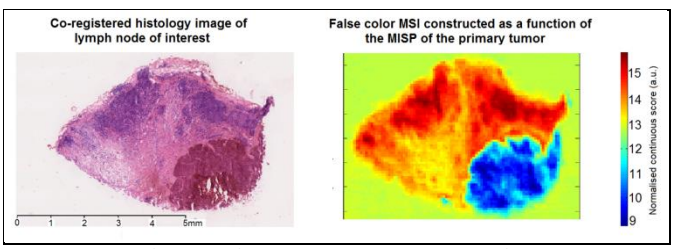

Figure 3: Identification of metastases in lymph node of interest based on primary tumor MISP.

In conclusion, we have demonstrated the first use of DESI-MSI for the identification of LNM and have shown that its metabolic profile is similar to that of the primary tumor in a single patient. We validated our findings by creating a RMMC multivariate statistical model based on the MISP of the primary tumor and identified metastases within a LN of interest.

This research was supported by the European Research Council under the Starting Grant scheme (contract no. 210356) and Imperial College Junior Fellowship Scheme.

Notes and references

1 C. A. Roberts, P. D. Beitsch, C. E. Litz, D. S. Hilton, G. E. Ewing, E. Clifford, W. Taylor, M. R. Hapke, A. Babaian, L. Khalid, J. D. Hall, G. Lindberg, K. Molberg and H. Saboorian, *Am. J. Surg.*, 2003, 186(4), 324-9.
2 M. Tsujimoto, K. Nakabayashi, K. Yoshidome, T. Kaneko, T. Iwase, F. Akiyama, Y. Kato, H. Tsuda, S. Ueda, K. Sato, Y. Tamaki, S. Noguchi, T. R. Kataoka, H. Nakajima, Y. Komoike, H. Inaji, K. Tsugawa, K. Suzuki, S. Nakamura, M. Daitoh, Y. Otomo and N. Matsuura, *Clin. Cancer Res.*, 2007, 13, 4807–16.

3 Nissan, D. Jager, M. Roystacher, D. Prus, T.Peretz, I.Eisenberg, H. R.Freund, M. Scanlan, G. Ritter, L. J. Old and S. Mitrani-Rosenbaum, *Br. J. Cancer*, 2006, 94, 681–685.
4 D. J. Grootendorst, J. Jose, W. M. Wouters, H. Van Bouven, J. Van der Hage, T. G. Van Leeuwen, W. Steenbergen, S. Manohar and T. J. Ruers, *Lasers Surg. Med*., 2012, 44(7), 541-9.
5 S. J. González, J. Wong, L. González, P. Brader, M. Zakowski, Y. Fong and V. E. Strong, *Surg. Endosc.*, 2011, 25(10), 3214-21.
6 J. Horsenell, P. Stonelake, J. Christie-Brown, G. Shetty, J. Hutchings, C. Kendall and N. Stone, *Analyst*, 2010, 135(12), 3042-7.
7 J. C. Vickerman, *Analyst*, 2011, 136(11), 2199-217.
8 E. H. Seeley and R. M. Caprioli, *Proteomics Clin. Appl.*, 2008, 2, 1435–1443.
9 W. M. Hardesty and R. M. Caprioli, *Anal. Bioanal. Chem.*, 2008, 391(3), 899–903.
10 D. Hare, F. Burger, C. Austin, F. Fryer, R. Grimm, B Reedy, R. A. Scolyer, J. F. Thompson, P. Doble, *Analyst*, 2009, 134(3), 450-3.
11 L. S. Eberlin, I. Norton, A. L. Dill, A.J. Golby, K. L. Ligon, S. Santagata, R. G. Cooks and N.Y. Agar, *Cancer Res*, 2012, 72(3), 645-54.
12 S. Gerbig, O. Golf, J. Balog, J. Denes, Z. Baranyai, A. Zarand, E. Raso, J. Timar and Z. Takats, *Anal. Bioanal. Chem.*, 2012, 403(8), 2315-25.
13 Z. Takats, J. M. Wiseman, B. Gologan, R. G. Cooks. *Science*, 2004, 306(5695), 471-3.
14 J. M. Wiseman, D. R. Ifa, A. Venter and R. G. Cooks, *Nat. Prot*., 2008, 3(3), 517-24.
15 K. A. Veselkov, R. Mirnezami, N. Strittmatter, R. D. Goldin, J. Kinross, A. Speller, T. Abramov, E. A. Jones. A. Darzi, E. Holmes, J. K. Nicholson and Takats Z. *PNAS*, in press.
16 J. A. Menendez and R. Lupu, Nat. Rev. *Cancer*, 2007, 7(10): 763-77.
17 J. Balog, L. Sasi-Szabo, J. Kinross, M. R. Lewis, L. J. Murihead, K. Veselkov, R. Mirnezami, B. Dezso, L. Damjanovich, A. Darzi, J.K. Nicholson, Z. Takats. Sci. Transl. Med., 2013, 5(194), 194ra93. doi: 10.1126/scitranslmed.3005623.194ra93.